# Convergence analysis of HDG formulations for the convected Helmholtz equation

Nathan Rouxelin, Hélène Barucq, Sébastien Tordeux

# Convergence analysis of HDG formulations for the convected Helmholtz equation

April 12-16th, 2021
ICOSAHOM 2020

Nathan ROUXELIN
nathan.rouxelin@inria.fr
Joint work with: H. Barucq, S. Tordeux

Inria Makutu – e2s-UPPA – LMAP

e2s UPPA
energy environment solutions

Inria

UNIVERSITÉ DE PAU ET DES PAYS DE L'ADOUR

# Context of this work



## Helioseismology in a nutshell:

- Aims at imaging the solar interior thanks to surface observations
- Surfacic «acoustic waves» can be measured thanks to relativistic Doppler effect
- The full models are too complicated for numerical simulation, two main approaches for computational heliosesimolgy:
  - Aeroacoustics: magnetic effects are neglected
  - Magnetoacoustics: hydrodynamics effects are neglected

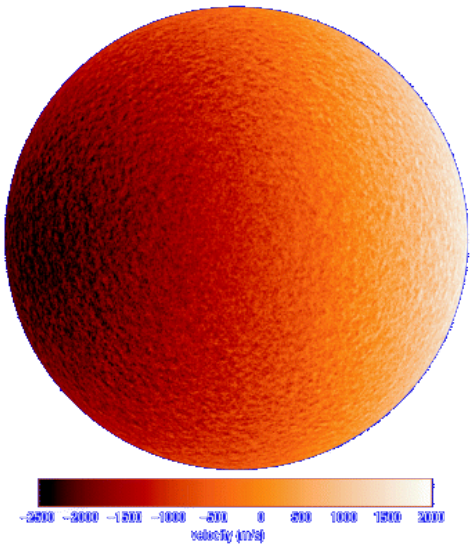

(a) Dopplergram

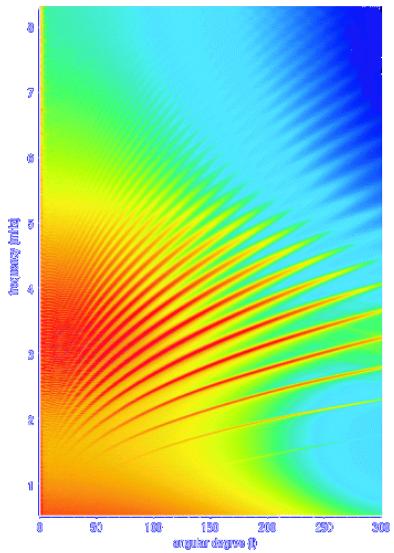

(b) Power spectrum

# Outline



1. What is HDG ?

2. HDG methods for the convected Helmholtz equation

3. Numerical results

# What is HDG ?

# From CG... to DG... to HDG



From CG to DG:

- Continuity of the solution between two elements is not enforced by the choice of approximation spaces anymore
- Continuity and stability come from the choice of numerical flux between two elements (similar to the finite volume method)
- Advantages
  - *hp*-adaptativity
  - high-order
  - parallelization
- Disadvantage
  - large number of degrees of freedom

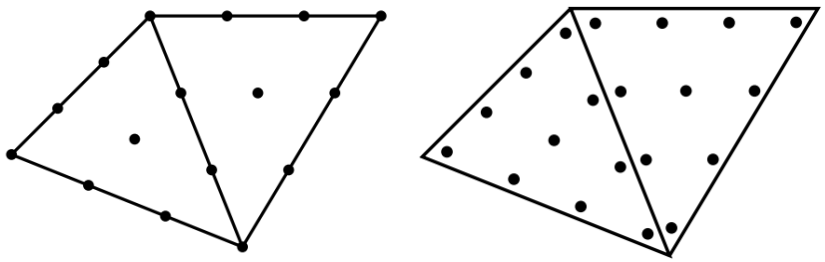

(c) CG (d) DG

Figure: Degrees of freedom for degree 3

# From CG... to DG... to HDG



From CG to DG:

- Continuity of the solution between two elements is not enforced by the choice of approximation spaces anymore
- Continuity and stability come from the choice of numerical flux between two elements (similar to the finite volume method)

From DG to HDG:

- Introduce a new unknown on the skeleton of the mesh
- Interior degrees of freedom can be eliminated through static condensation
- Keep the advantages of DG for a reduced cost

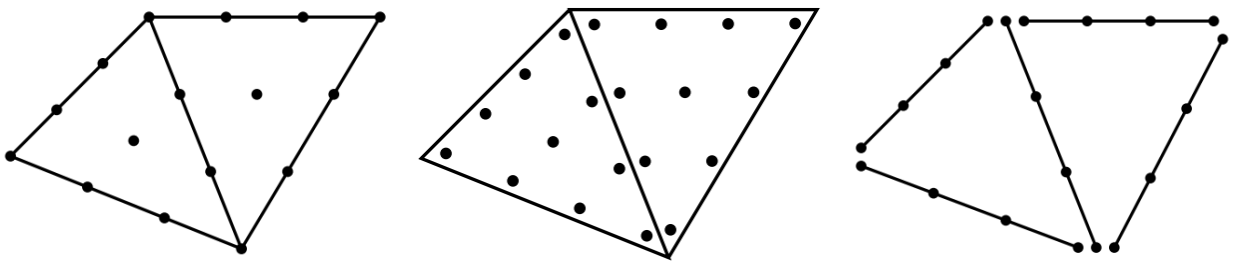

(a) CG (b) DG (c) HDG

Figure: Degrees of freedom for degree 3

# From CG... to DG... to HDG



From CG to DG:

- Continuity of the solution between two elements is not enforced by the choice of approximation spaces anymore
- Continuity and stability come from the choice of numerical flux between two elements (similar to the finite volume method)

From DG to HDG:

- Introduce a new unknown on the skeleton of the mesh
- Interior degrees of freedom can be eliminated through static condensation
- Keep the advantages of DG for a reduced cost

HDG methods have a dual citizenship:

- Static condensation of DG methods
- Also related to the hybridization of mixed FEM (*eg* Raviart-Thomas or Brezzi-Douglas-Marini methods)

# HDG methods for the convected Helmholtz equation

# Convected Helmholtz equation



Model problem :

$$\rho_0 \left(-\omega^2 p - 2i\omega \boldsymbol{v_0} \cdot \nabla p + \boldsymbol{v_0} \cdot \nabla(\boldsymbol{v_0} \cdot \nabla p)\right) - \operatorname{div}\left(\rho_0 {c_0}^2 \nabla p\right) = s$$

where

- $p$: acoustic potential ($\sim$ pressure perturbation)
- $\rho_0$: mass density
- $\boldsymbol{v_0}$: velocity field
- $c_0$: sound speed
- $s$: acoustic source

# Convected Helmholtz equation



Model problem :

$$\rho_0 \left(-\omega^2 p - 2i\omega \boldsymbol{v_0} \cdot \nabla p\right) - \operatorname{div}\left(\boldsymbol{M_0} \nabla p\right) = s$$

where $\boldsymbol{M_0} = \rho_0 {c_0}^2 \mathrm{Id} - \rho_0 \boldsymbol{v_0} {\boldsymbol{v_0}}^T$.

# Convected Helmholtz equation



Model problem :

- Choice 1: *diffusive flux*

$$\boldsymbol{W_0 q} + \nabla p = 0,$$
$$-\rho_0 \omega^2 p - 2i\omega\rho_0 \boldsymbol{v_0} \cdot \nabla p + \operatorname{div}(\boldsymbol{q}) = s$$

  where $\boldsymbol{q} = -\boldsymbol{M_0}\nabla p$ and $\boldsymbol{W_0} = \boldsymbol{M_0}^{-1}$.

- Choice 2: *total flux*

$$\boldsymbol{W_0 \sigma} + \nabla p + 2i\omega p \boldsymbol{W_0} \rho_0 \boldsymbol{v_0} = 0,$$
$$-\rho_0 \omega^2 p + \operatorname{div}(\boldsymbol{\sigma}) = s,$$

  where $\boldsymbol{\sigma} = -\boldsymbol{M_0}\nabla p - 2i\omega p \rho_0 \boldsymbol{v_0}$.

To use HDG methods, we need a first-order in space formulation.

# Convected Helmholtz equation



Model problem :

Seek $(\boldsymbol{q}, p) \in \boldsymbol{H}_{\text{div}}(\Omega) \times H^1(\Omega)$ such that

$$\int_\Omega \boldsymbol{W_0 q} \cdot \boldsymbol{r}^* \mathrm{d}x - \int_\Omega p \mathrm{div}\,(\boldsymbol{r}^*)\,\mathrm{d}x + \int_{\partial\Omega} p \boldsymbol{r}^* \cdot \boldsymbol{n} \mathrm{d}\sigma = 0$$

$$-\omega^2 \int_\Omega \rho_0 p w^* \mathrm{d}x + 2i\omega \int_\Omega p \rho_0 \boldsymbol{v_0} \cdot \nabla w^* \mathrm{d}x$$

$$-\int_\Omega \boldsymbol{q} \cdot \nabla w^* \mathrm{d}x + \int_{\partial\Omega} w^* \boldsymbol{q} \cdot \boldsymbol{n} - 2i\omega p w^* \rho_0 \boldsymbol{v_0} \cdot \boldsymbol{n} \mathrm{d}\sigma = \int_\Omega s w^* \mathrm{d}x$$

for all $(\boldsymbol{r}, w) \in \boldsymbol{H}_{\text{div}}(\Omega) \times H^1(\Omega)$.

Very similar if we use $\boldsymbol{\sigma}$ instead of $\boldsymbol{q}$.

# Convected Helmholtz equation



Model problem :

Seek $(\boldsymbol{q}, p) \in \boldsymbol{H}_{\text{div}}(\Omega) \times H^1(\Omega)$ such that

$$\int_\Omega \boldsymbol{W_0 q} \cdot \boldsymbol{r}^* \mathrm{d}x - \int_\Omega p \mathrm{div}\,(\boldsymbol{r}^*)\,\mathrm{d}x + \int_{\partial\Omega} p \boldsymbol{r}^* \cdot \boldsymbol{n} \mathrm{d}\sigma = 0$$

$$-\omega^2 \int_\Omega \rho_0 p w^* \mathrm{d}x + 2i\omega \int_\Omega p \rho_0 \boldsymbol{v_0} \cdot \nabla w^* \mathrm{d}x$$

$$-\int_\Omega \boldsymbol{q} \cdot \nabla w^* \mathrm{d}x + \int_{\partial\Omega} w^* \boldsymbol{q} \cdot \boldsymbol{n} - 2i\omega p w^* \rho_0 \boldsymbol{v_0} \cdot \boldsymbol{n} \mathrm{d}\sigma = \int_\Omega s w^* \mathrm{d}x$$

for all $(\boldsymbol{r}, w) \in \boldsymbol{H}_{\text{div}}(\Omega) \times H^1(\Omega)$.

Well-posedness:

- if the carrier flow is subsonic

$$\inf_\Omega \left( {c_0}^2 - |\boldsymbol{v_0}|^2 \right) > 0$$

  then the problem is of Fredholm type
- uniqueness of the solution comes from the boundary conditions.

Skeleton unknown: numerical trace $\lambda_h$ approximates $p$ on $\mathcal{E}_h$.

$$\int_{\partial K} p\boldsymbol{r}^* \cdot \boldsymbol{n} \mathrm{d}\sigma \xrightarrow{\text{discretization}} \int_{\partial K} \lambda_h \boldsymbol{r}^* \cdot \boldsymbol{n} \mathrm{d}\sigma$$

# HDG(+) methods
## Approximation spaces



Skeleton unknown: numerical trace $\lambda_h$ approximates $p$ on $\mathcal{E}_h$.

$$\int_{\partial K} p\boldsymbol{r}^* \cdot \boldsymbol{n} \mathrm{d}\sigma \xrightarrow{\text{discretization}} \int_{\partial K} \lambda_h \boldsymbol{r}^* \cdot \boldsymbol{n} \mathrm{d}\sigma$$

Approximation spaces:

| Unknown | Space | HDG | HDG+ |
|---|---|---|---|
| Pressure $p_h$ | $W_h(K)$ | $\mathcal{P}_k(K)$ | $\mathcal{P}_{k+1}(K)$ |
| Flux $\boldsymbol{q}_h/\boldsymbol{\sigma}_h$ | $\boldsymbol{V}_h(K)$ | $\boldsymbol{\mathcal{P}}_k(K)$ | |
| Trace $\lambda_h$ | $M_h(e)$ | $\mathcal{P}_k(e)$ | |

Warning: HDG+ only works in $(\boldsymbol{q}, p)$ formulation !

We will compare the HDG-$\boldsymbol{q}_h$, HDG-$\boldsymbol{\sigma}_h$ and HDG+ methods for time-harmonic convected waves.

# HDG(+) methods
## Approximation spaces



Skeleton unknown: numerical trace $\lambda_h$ approximates $p$ on $\mathcal{E}_h$.

$$\int_{\partial K} p\boldsymbol{r}^* \cdot \boldsymbol{n} \mathrm{d}\sigma \xrightarrow{\text{discretization}} \int_{\partial K} \lambda_h \boldsymbol{r}^* \cdot \boldsymbol{n} \mathrm{d}\sigma$$

Approximation spaces:

| Unknown | Space | HDG | HDG+ |
|---|---|---|---|
| Pressure $p_h$ | $W_h(K)$ | $\mathcal{P}_k(K)$ | $\mathcal{P}_{k+1}(K)$ |
| Flux $\boldsymbol{q}_h/\boldsymbol{\sigma}_h$ | $\boldsymbol{V}_h(K)$ | $\boldsymbol{\mathcal{P}}_k(K)$ | |
| Trace $\lambda_h$ | $M_h(e)$ | $\mathcal{P}_k(e)$ | |

Together with the weak formulation: leads to the discrete local problem (*ie* on an element $K \in \mathcal{T}_h$) :

$$\mathbb{A}^K \begin{bmatrix} {p_h}^K \\ {\boldsymbol{q}_h}^K \end{bmatrix} + \mathbb{C}^K \left[ {\lambda_h}^K \right] = \mathbb{S}^K$$

# HDG(+) methods
## Numerical flux and transmission condition



At this point:

- The approximation spaces are discontinuous.
- We need to enforce the continuity of the numerical solution between the elements.
- We need to ensure the stability of the method.

At this point:

- The approximation spaces are discontinuous.
- We need to enforce the continuity of the numerical solution between the elements.
- We need to ensure the stability of the method.

All of this is done by choosing the numerical flux, so that

$$\sum_{e\in\mathcal{E}_h}\int_e [\![\widehat{\boldsymbol{q}_h} - 2i\omega \boldsymbol{n}\cdot\widehat{\boldsymbol{v}_0 p_h}\boldsymbol{n}]\!]\mu^*\,\mathrm{d}\sigma = 0, \quad \text{or} \quad \sum_{e\in\mathcal{E}_h}\int_e [\![\widehat{\boldsymbol{\sigma}_h}]\!]\mu^*\,\mathrm{d}\sigma = 0,$$

for all $\mu \in M_h$ and where $[\![\cdot]\!]$ is the DG-jump operator.

All of this is done by choosing the numerical flux, so that

$$\sum_{e\in\mathcal{E}_h}\int_e [\![\widehat{\boldsymbol{q}_h} - 2i\omega \boldsymbol{n}\cdot\widehat{\boldsymbol{v}_0 p_h}\boldsymbol{n}]\!]\mu^*\,\mathrm{d}\sigma = 0, \quad \text{or} \quad \sum_{e\in\mathcal{E}_h}\int_e [\![\widehat{\boldsymbol{\sigma}_h}]\!]\mu^*\,\mathrm{d}\sigma = 0,$$

for all $\mu \in M_h$ and where $[\![\cdot]\!]$ is the DG-jump operator.

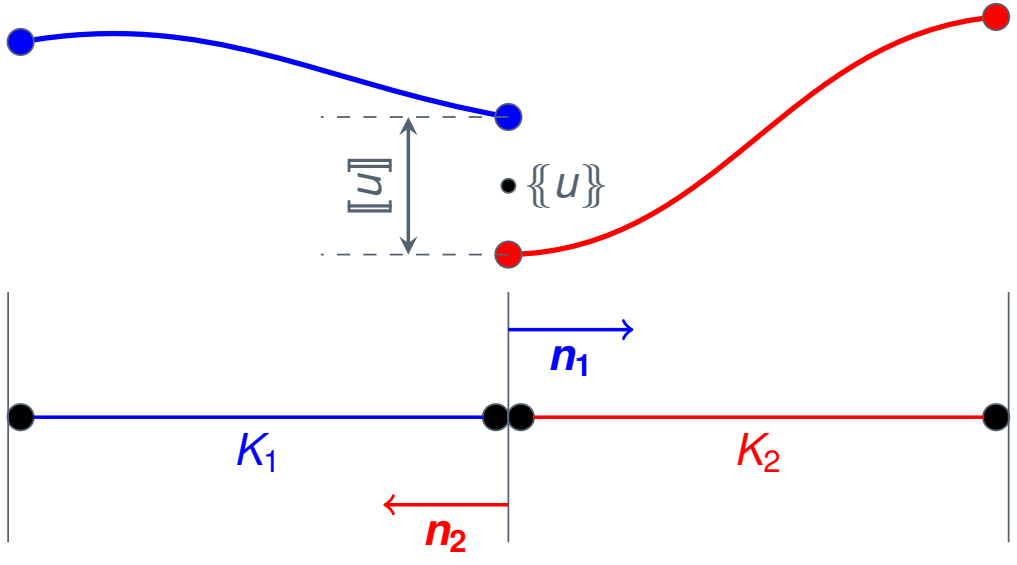


Figure: Discontinuity between two elements


All of this is done by choosing the numerical flux, so that

$$\sum_{e\in\mathcal{E}_h}\int_e [\![\widehat{\boldsymbol{q}_h} - 2i\omega \boldsymbol{n}\cdot\widehat{\boldsymbol{v}_0 p_h}\boldsymbol{n}]\!]\mu^*\,\mathrm{d}\sigma = 0, \quad \text{or} \quad \sum_{e\in\mathcal{E}_h}\int_e [\![\widehat{\boldsymbol{\sigma}_h}]\!]\mu^*\,\mathrm{d}\sigma = 0,$$

for all $\mu \in M_h$ and where $[\![\cdot]\!]$ is the DG-jump operator.

Numerical flux:

$$\widehat{\boldsymbol{q}_h}^K\cdot\boldsymbol{n} - 2i\omega\widehat{p_h{}^K\boldsymbol{v}_0}\cdot\boldsymbol{n} = \boldsymbol{q}_h{}^K\cdot\boldsymbol{n} - 2i\omega(\boldsymbol{v}_0\cdot\boldsymbol{n})\lambda_h{}^K + 2i\omega\tau\left(\mathrm{P}_k p_h{}^K - \lambda_h{}^K\right)$$

$$\widehat{\boldsymbol{\sigma}_h}^K\cdot\boldsymbol{n} = \boldsymbol{\sigma}_h{}^K\cdot\boldsymbol{n} + i\omega\tau(p_h{}^K - \lambda_h{}^K)$$

where

- $\tau$: penalization parameter
- $\mathrm{P}_k$: $L^2$-projection from $\mathcal{P}_{k+1}(e)$ to $\mathcal{P}_k(e)$

All of this is done by choosing the numerical flux, so that

$$\sum_{e\in\mathcal{E}_h}\int_e [\![\widehat{\boldsymbol{q}_h} - 2i\omega \boldsymbol{n}\cdot\widehat{\boldsymbol{v}_0 p_h}\boldsymbol{n}]\!]\mu^* \mathrm{d}\sigma = 0, \quad \text{or} \quad \sum_{e\in\mathcal{E}_h}\int_e [\![\widehat{\boldsymbol{\sigma}_h}]\!]\mu^* \mathrm{d}\sigma = 0,$$

for all $\mu \in M_h$ and where $[\![\cdot]\!]$ is the DG-jump operator.

Numerical flux:

$$\widehat{\boldsymbol{q}_h}^K \cdot \boldsymbol{n} - 2i\omega\widehat{p_h{}^K \boldsymbol{v}_0}\cdot\boldsymbol{n} = \boldsymbol{q}_h{}^K\cdot\boldsymbol{n} - 2i\omega(\boldsymbol{v}_0\cdot\boldsymbol{n})\lambda_h{}^K + 2i\omega\tau\left(\mathrm{P}_k p_h{}^K - \lambda_h{}^K\right)$$

$$\widehat{\boldsymbol{\sigma}_h}^K\cdot\boldsymbol{n} = \boldsymbol{\sigma}_h{}^K\cdot\boldsymbol{n} + i\omega\tau(p_h{}^K - \lambda_h{}^K)$$

This leads to the discrete transmission condition:

$$\sum_{K\in\mathcal{T}_h}\left(\mathbb{B}^K\begin{bmatrix} p_h{}^K \\ \boldsymbol{q}_h{}^K\end{bmatrix} + \mathbb{L}^K\left[\lambda_h{}^K\right]\right) = 0$$

Recall from the previous slides:

- Local problem on $K \in \mathcal{T}_h$

$$\mathbb{A}^K \begin{bmatrix} {p_h}^K \\ {\boldsymbol{q}_h}^K \end{bmatrix} + \mathbb{C}^K \left[ {\lambda_h}^K \right] = \mathbb{S}^K$$

- Transmission condition

$$\sum_{K \in \mathcal{T}_h} \left( \mathbb{B}^K \begin{bmatrix} {p_h}^K \\ {\boldsymbol{q}_h}^K \end{bmatrix} + \mathbb{L}^K \left[ {\lambda_h}^K \right] \right) = 0$$

Recall from the previous slides:

- Local problem on $K \in \mathcal{T}_h$

$$\mathbb{A}^K \begin{bmatrix} {p_h}^K \\ {\boldsymbol{q}_h}^K \end{bmatrix} + \mathbb{C}^K \left[ {\lambda_h}^K \right] = \mathbb{S}^K \Longrightarrow \begin{bmatrix} {p_h}^K \\ {\boldsymbol{q}_h}^K \end{bmatrix} = (\mathbb{A}^K)^{-1}\mathbb{S}^K - (\mathbb{A}^K)^{-1}\mathbb{C}^K \left[ {\lambda_h}^K \right]$$

- Transmission condition

$$\sum_{K \in \mathcal{T}_h} \left( \mathbb{B}^K \begin{bmatrix} {p_h}^K \\ {\boldsymbol{q}_h}^K \end{bmatrix} + \mathbb{L}^K \left[ {\lambda_h}^K \right] \right) = 0$$

Dimensions of the unknowns: Notice that

$\begin{bmatrix} {p_h}^K \\ {\boldsymbol{q}_h}^K \end{bmatrix}$ is volumetric and $\left[ {\lambda_h}^K \right]$ is surfacic.

## Recall from the previous slides:

- Local problem on $K \in \mathcal{T}_h$

$$\mathbb{A}^K \begin{bmatrix} {p_h}^K \\ {\boldsymbol{q}_h}^K \end{bmatrix} + \mathbb{C}^K \left[ {\lambda_h}^K \right] = \mathbb{S}^K \Longrightarrow \begin{bmatrix} {p_h}^K \\ {\boldsymbol{q}_h}^K \end{bmatrix} = (\mathbb{A}^K)^{-1}\mathbb{S}^K - (\mathbb{A}^K)^{-1}\mathbb{C}^K \left[ {\lambda_h}^K \right]$$

- Transmission condition

$$\sum_{K \in \mathcal{T}_h} \left( \mathbb{B}^K \begin{bmatrix} {p_h}^K \\ {\boldsymbol{q}_h}^K \end{bmatrix} + \mathbb{L}^K \left[ {\lambda_h}^K \right] \right) = 0$$

## Static condensation:

$$\mathbb{M}\left[\lambda_h\right] = \mathbb{S} \quad \underset{\text{reconstruction}}{\overset{\text{elimination}}{\longleftrightarrow}} \quad \begin{bmatrix} {p_h}^K \\ {\boldsymbol{q}_h}^K \end{bmatrix} = (\mathbb{A}^K)^{-1}\mathbb{S}^K - (\mathbb{A}^K)^{-1}\mathbb{C}^K \left[ {\lambda_h}^K \right],$$

with

$$\mathbb{M} := \sum_{K \in \mathcal{T}_h} \left( \mathbb{L}^K - \mathbb{B}^K (\mathbb{A}^K)^{-1} \mathbb{C}^K \right) \quad \text{and} \quad \mathbb{S} := -\sum_{K \in \mathcal{T}_h} \mathbb{B}^K (\mathbb{A}^K)^{-1} \mathbb{S}^K$$

# Some results on the methods



We performed the numerical analysis of the method:

- **Local solvability:** $\mathbb{A}^K$ is invertible if
  - $\omega h_K < C(\rho_0, \boldsymbol{v_0}, c_0, \text{element geometry})$,
  - $\tau$ is well chosen

# Some results on the methods



We performed the numerical analysis of the method:

- **Local solvability:** $\mathbb{A}^K$ is invertible if
  - $\omega h_K < C(\rho_0, \boldsymbol{v_0}, c_0, \text{element geometry})$,
  - $\tau$ is well chosen
    - for HDG-$\boldsymbol{\sigma}_h$: optimal choice can be computed *a priori*,
    - for HDG+: large and not very sensitive,
    - for HDG-$\boldsymbol{q}_h$: small and quite sensitive.

# Some results on the methods



We performed the numerical analysis of the method:

- **Local solvability:** $\mathbb{A}^K$ is invertible if
  - $\omega h_K < C(\rho_0, \boldsymbol{v_0}, c_0, \text{element geometry})$,
  - $\tau$ is well chosen
    - for HDG-$\boldsymbol{\sigma}_h$: optimal choice can be computed *a priori*,
    - for HDG+: large and not very sensitive,
    - for HDG-$\boldsymbol{q}_h$: small and quite sensitive.
- **Global solvability:** $\mathbb{M}$ is invertible if $\omega \notin \mathcal{R}$, where

$$\mathcal{R} := \{\omega \mid \text{continuous problem not uniquely solvable}\}$$

is the set of *resonant frequencies*.

# Error analysis of the HDG+ method



Error quantities:

$$\varepsilon_h^{\boldsymbol{q}} := \boldsymbol{q}_h - \boldsymbol{\Pi}\boldsymbol{q}, \quad \varepsilon_h^{p} := p_h - \Pi p, \quad \widehat{\varepsilon}_h^{p} := \lambda_h - \mathrm{P}_k p,$$

where $\boldsymbol{\Pi}$, $\Pi$ and $\mathrm{P}_k$ are $L^2$-projections onto the approximation spaces $\boldsymbol{V}_h$, $W_h$ and $M_h$.

# Error analysis of the HDG+ method



Error quantities:

$$\varepsilon_h^{\boldsymbol{q}} := \boldsymbol{q}_h - \boldsymbol{\Pi}\boldsymbol{q}, \quad \varepsilon_h^{p} := p_h - \Pi p, \quad \widehat{\varepsilon}_h^{p} := \lambda_h - \mathrm{P}_k p,$$

where $\boldsymbol{\Pi}$, $\Pi$ and $\mathrm{P}_k$ are $L^2$-projections onto the approximation spaces $\boldsymbol{V}_h$, $W_h$ and $M_h$.

Main steps of the analysis:

- **Step 1:** Energy-like estimate

$$\left| \left\| \varepsilon_h^{\boldsymbol{q}} \right\|^2 - 2i\omega \left\| \mathrm{P}_k \varepsilon_h^{p} - \widehat{\varepsilon}_h^{p} \right\|_{\partial \mathcal{T}_h}^2 \right| \lesssim F\left( \left\| \varepsilon_h^{\boldsymbol{q}} \right\|, \left\| \varepsilon_h^{p} \right\|, \left\| \mathrm{P}_k \varepsilon_h^{p} - \widehat{\varepsilon}_h^{p} \right\|_{\partial \mathcal{T}_h} \right)$$

# Error analysis of the HDG+ method



Error quantities:

$$\varepsilon_h^{\boldsymbol{q}} := \boldsymbol{q}_h - \boldsymbol{\Pi}\boldsymbol{q}, \quad \varepsilon_h^p := p_h - \Pi p, \quad \widehat{\varepsilon}_h^p := \lambda_h - \mathrm{P}_k p,$$

where $\boldsymbol{\Pi}$, $\Pi$ and $\mathrm{P}_k$ are $L^2$-projections onto the approximation spaces $\boldsymbol{V}_h$, $W_h$ and $M_h$.

Main steps of the analysis:

- **Step 1:** Energy-like estimate

$$\left| \left\| \varepsilon_h^{\boldsymbol{q}} \right\|^2 - 2i\omega \left\| \mathrm{P}_k \varepsilon_h^p - \widehat{\varepsilon}_h^p \right\|_{\partial \mathcal{T}_h}^2 \right| \lesssim F\left( \left\| \varepsilon_h^{\boldsymbol{q}} \right\|, \left\| \varepsilon_h^p \right\|, \left\| \mathrm{P}_k \varepsilon_h^p - \widehat{\varepsilon}_h^p \right\|_{\partial \mathcal{T}_h} \right)$$

- **Step 2:** Dual estimate

$$\left\| \varepsilon_h^p \right\| \lesssim \omega h \cdot G\left( \left\| \varepsilon_h^{\boldsymbol{q}} \right\|, \left\| \mathrm{P}_k \varepsilon_h^p - \widehat{\varepsilon}_h^p \right\|_{\partial \mathcal{T}_h} \right)$$

# Error analysis of the HDG+ method



Error quantities:

$$\varepsilon_h^{\boldsymbol{q}} := \boldsymbol{q}_h - \boldsymbol{\Pi}\boldsymbol{q}, \quad \varepsilon_h^{p} := p_h - \Pi p, \quad \widehat{\varepsilon}_h^{p} := \lambda_h - \mathrm{P}_k p,$$

where $\boldsymbol{\Pi}$, $\Pi$ and $\mathrm{P}_k$ are $L^2$-projections onto the approximation spaces $\boldsymbol{V}_h$, $W_h$ and $M_h$.

Main steps of the analysis:

- **Step 1:** Energy-like estimate

$$\left| \left\| \varepsilon_h^{\boldsymbol{q}} \right\|^2 - 2i\omega \left\| \mathrm{P}_k \varepsilon_h^{p} - \widehat{\varepsilon}_h^{p} \right\|_{\partial \mathcal{T}_h}^2 \right| \lesssim F\left( \left\| \varepsilon_h^{\boldsymbol{q}} \right\|, \left\| \varepsilon_h^{p} \right\|, \left\| \mathrm{P}_k \varepsilon_h^{p} - \widehat{\varepsilon}_h^{p} \right\|_{\partial \mathcal{T}_h} \right)$$

- **Step 2:** Dual estimate

$$\left\| \varepsilon_h^{p} \right\| \lesssim \omega h \cdot G\left( \left\| \varepsilon_h^{\boldsymbol{q}} \right\|, \left\| \mathrm{P}_k \varepsilon_h^{p} - \widehat{\varepsilon}_h^{p} \right\|_{\partial \mathcal{T}_h} \right)$$

- **Step 3:** Bootstrapping process

$$\left\| \varepsilon_h^{\boldsymbol{q}} \right\| = \mathcal{O}(h^{k+1}), \quad \left\| \varepsilon_h^{p} \right\| = \mathcal{O}(h^{k+2})$$

# Error analysis of the HDG+ method



**Summary of convergence rates:** $(\boldsymbol{q}, p)$ : exact solution

- for HDG-$\boldsymbol{q}_h$: (optimal ✗)

$$\|p_h - \Pi p\| = \mathcal{O}(h^{k+\frac{3}{2}}) \quad \text{and} \quad \|\boldsymbol{q}_h - \boldsymbol{\Pi}\boldsymbol{q}\| = \mathcal{O}(h^{k+\frac{1}{2}})$$

- for HDG-$\boldsymbol{\sigma}_h$: (optimal ✓)

$$\|p_h - \Pi p\| = \mathcal{O}(h^{k+1}) \quad \text{and} \quad \|\boldsymbol{\sigma}_h - \boldsymbol{\Pi}\boldsymbol{\sigma}\| = \mathcal{O}(h^{k+1})$$

- for HDG+: (optimal ✓)

$$\|p_h - \Pi p\| = \mathcal{O}(h^{k+2}) \quad \text{and} \quad \|\boldsymbol{q}_h - \boldsymbol{\Pi}\boldsymbol{q}\| = \mathcal{O}(h^{k+1})$$

# Error analysis of the HDG+ method



**Summary of convergence rates:** $(\boldsymbol{q}, p)$ : exact solution

- for HDG-$\boldsymbol{q}_h$: (optimal ✗) no super-convergence !

$$\|p_h - \Pi p\| = \mathcal{O}(h^{k+\frac{3}{2}}) \quad \text{and} \quad \|\boldsymbol{q}_h - \boldsymbol{\Pi}\boldsymbol{q}\| = \mathcal{O}(h^{k+\frac{1}{2}})$$

- for HDG-$\boldsymbol{\sigma}_h$: (optimal ✓) no super-convergence !

$$\|p_h - \Pi p\| = \mathcal{O}(h^{k+1}) \quad \text{and} \quad \|\boldsymbol{\sigma}_h - \boldsymbol{\Pi}\boldsymbol{\sigma}\| = \mathcal{O}(h^{k+1})$$

- for HDG+: (optimal ✓)

$$\|p_h - \Pi p\| = \mathcal{O}(h^{k+2}) \quad \text{and} \quad \|\boldsymbol{q}_h - \boldsymbol{\Pi}\boldsymbol{q}\| = \mathcal{O}(h^{k+1})$$

using:

- $L^2$-orthogonal projections for HDG-$\boldsymbol{q}_h$ and HDG+,
- tailored HDG projections for HDG-$\boldsymbol{\sigma}_h$.

# Numerical results

# Convergence



We work with relative $L^2$-errors

$$\mathcal{E}_p = \frac{\|p_h - \Pi p\|_{\mathcal{T}_h}}{\|\Pi p\|_{\mathcal{T}_h}}.$$

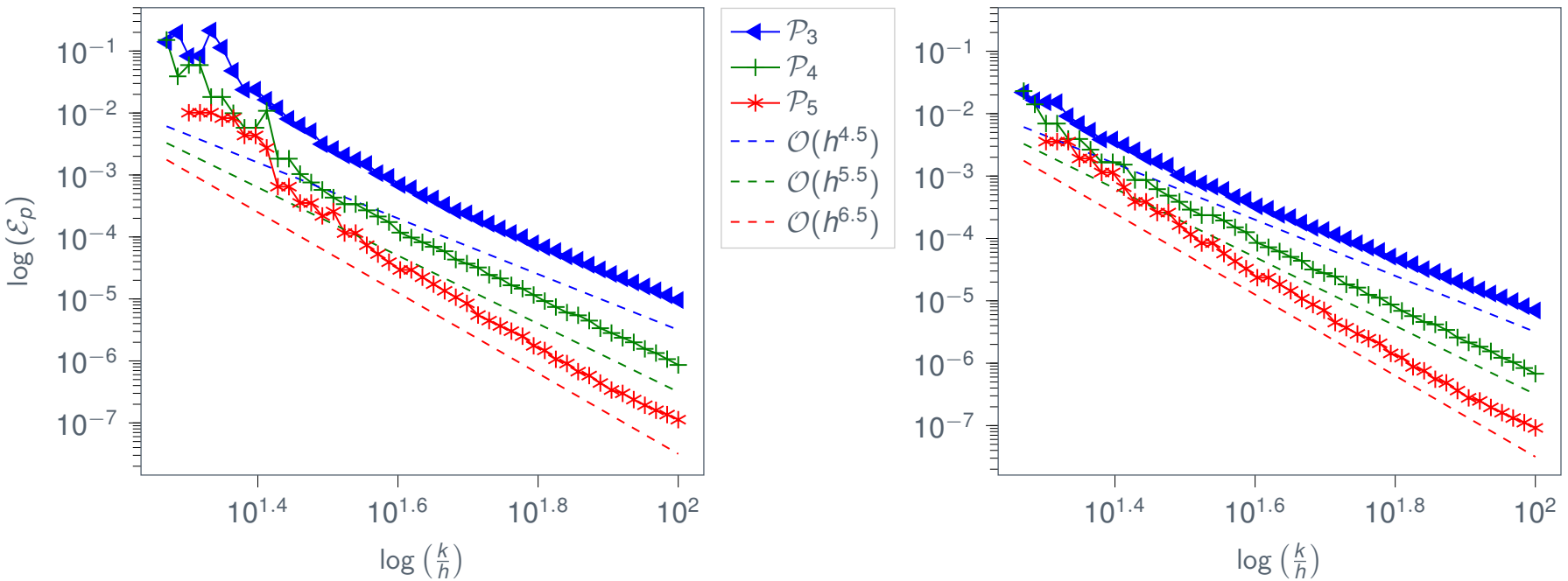


(a) HDG-$\boldsymbol{q}_h$ (b) HDG-$\boldsymbol{\sigma}_h$

Figure: Convergence for $p_h$ at Mach 0.4

# Convergence



We work with relative $L^2$-errors

$$\mathcal{E}_p = \frac{\|p_h - \Pi p\|_{\mathcal{T}_h}}{\|\Pi p\|_{\mathcal{T}_h}}.$$

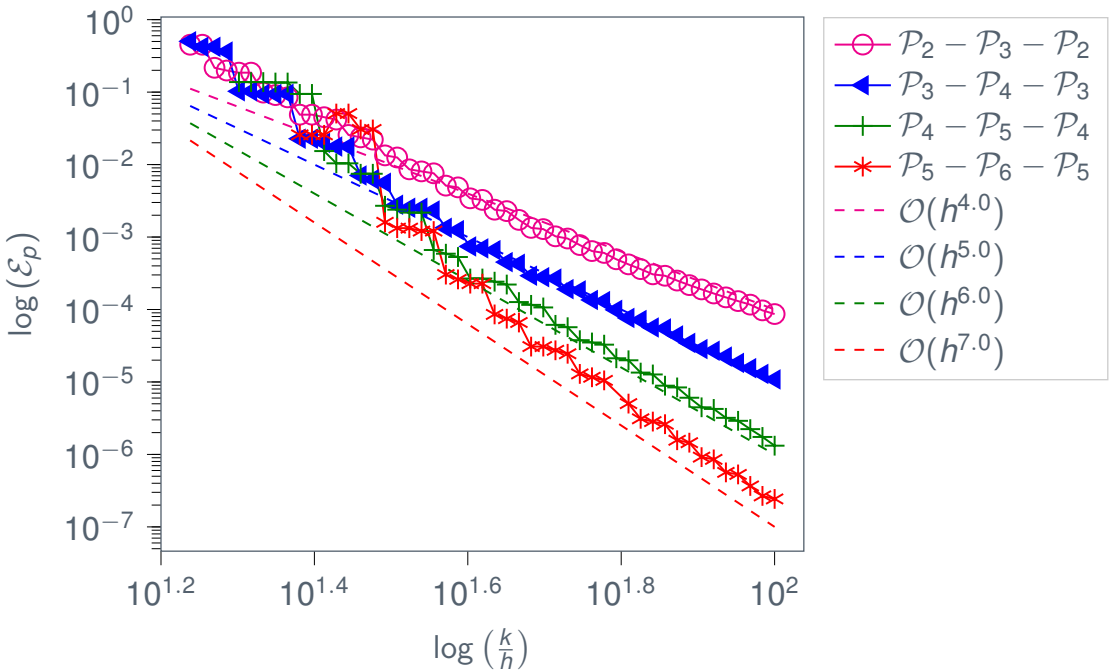


(a) HDG+

Figure: Convergence for $p_h$ at Mach 0.4

# Illustrative examples



Uniform flow:

$$\boldsymbol{v_0} = 0.6 \begin{bmatrix} \cos \frac{\pi}{4} \\ \sin \frac{\pi}{4} \end{bmatrix}$$

Validation: analytic solution for (a).

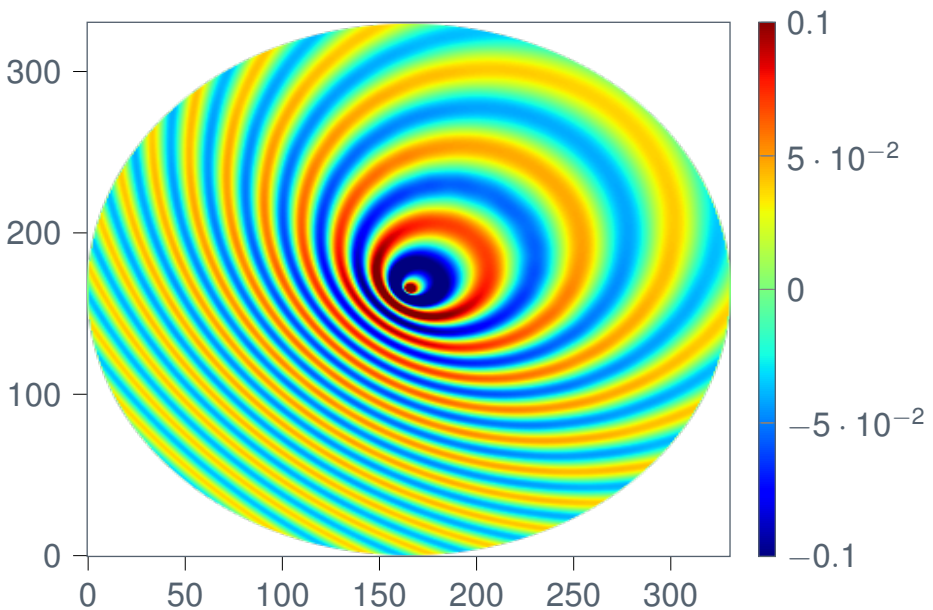


(a) One point-source

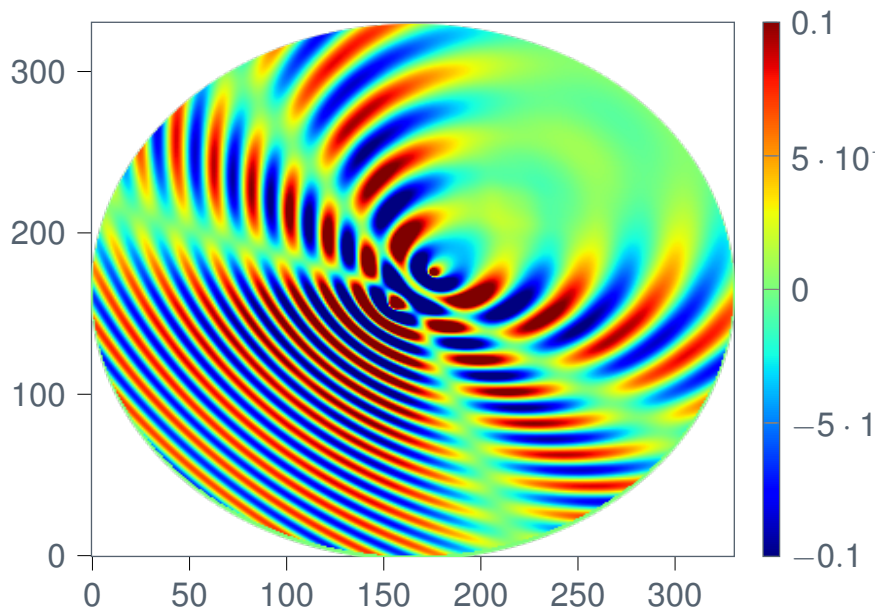


(b) Two point-sources

Figure: Numerical experiments using HDG-$\boldsymbol{\sigma}_h$

# Illustrative examples



Gaussian jet:

$$\boldsymbol{v_0} = M_0(y)\boldsymbol{e}_x, \quad \text{where} \quad M_0(y) := 0.1 + 0.3\exp\left(-\frac{y^2}{0.3^2}\right)$$

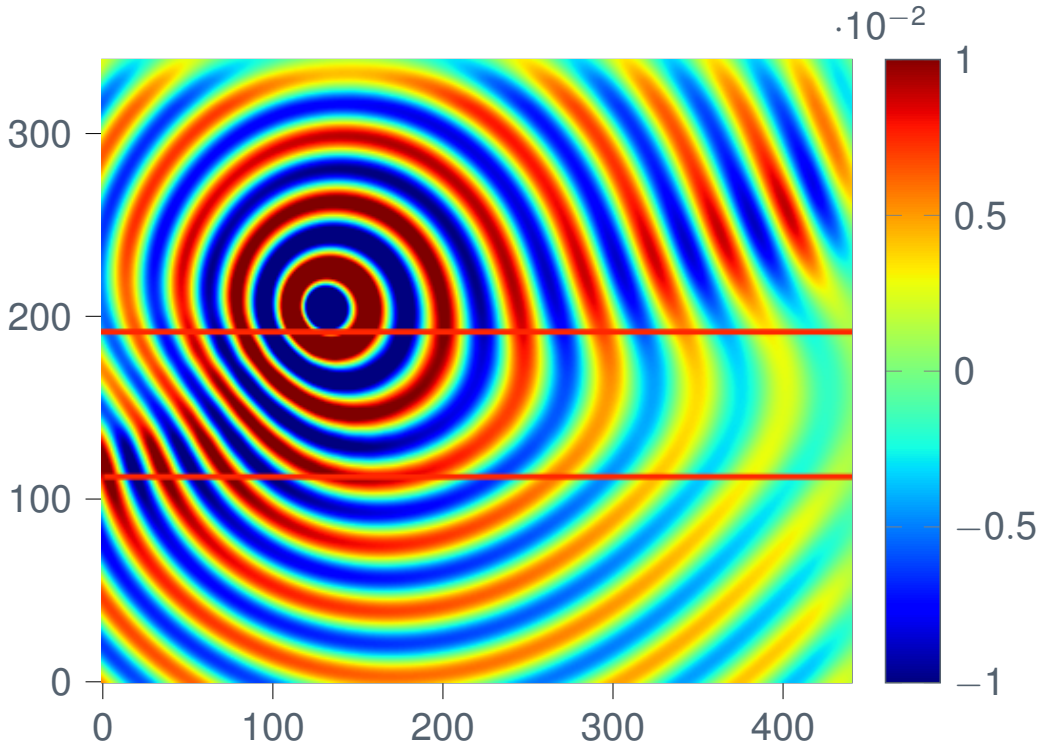


Figure: Point source in a jet-flow using HDG+

# Illustrative examples



Potential flow around a circular obstacle:

$$\boldsymbol{v_0} = M_\infty \left[ \left( 1 - \frac{R_C^2}{r^2} \right) \cos\theta \boldsymbol{e}_r + \left( 1 + \frac{R_C^2}{r^2} \right) \sin\theta \boldsymbol{e}_\theta \right],$$

where $R_C$ is the radius of the obstacle and $M_\infty$ the Mach number at infinity.

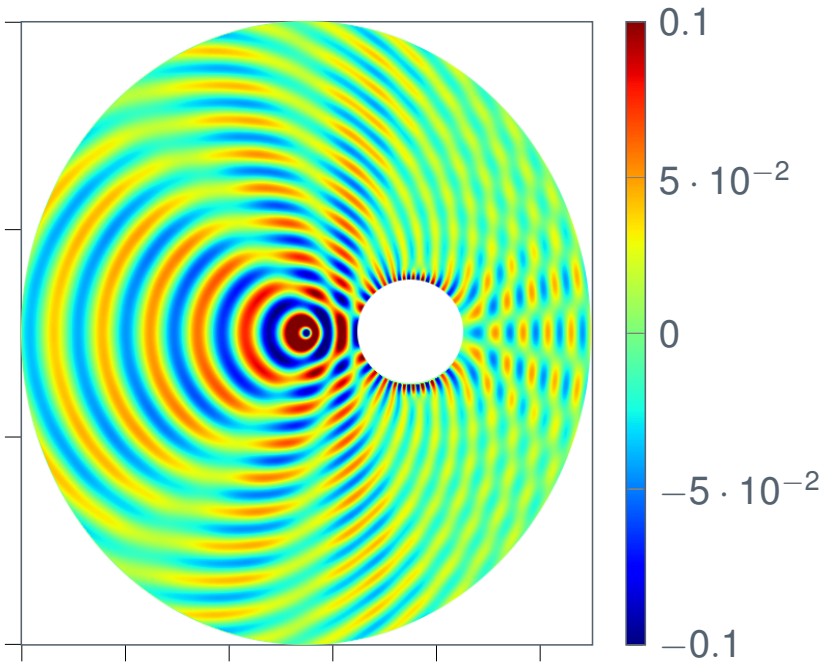


Figure: Point source in a potential flow around an obstacle using HDG-$\boldsymbol{\sigma}_h$

# Conclusion



Which method should we use ?

- HDG+
- HDG-$\boldsymbol{\sigma}_h$

as they are

- less sensitive to the choice of $\tau$,
- more robust with high Mach numbers,

than HDG-$\boldsymbol{q}_h$.

If you want to know more: a detailed pre-print is available

H. Barucq, N. Rouxelin, S. Tordeux.
*HDG and HDG+ methods for harmonic wave problems with convection*.
https://hal.inria.fr/hal-03253415

# References




H. Barucq, N. Rouxelin, S. Tordeux.
*HDG and HDG+ methods for harmonic wave problems with convection*.
https://hal.inria.fr/hal-03253415

FJ. Sayas, S. Du.
*An invitation to the theory of HDG methods*.
DOI:10.1007/978-3-030-27230-2

A. Hungria.
*Using HDG+ to Compute Solutions of the 3D Linear Elastic and Poroelastic Wave Equations*.
PhD Thesis - University of Delaware

C. Lehrenfeld.
*Hybrid Discontinuous Galerkin methods for solving incompressible flow problems*.
Thesis - RWTH Aachen

B. Cockburn, J. Gopalakrishnan, FJ. Sayas.
*A projection-based error analysis of HDG methods*.
DOI:10.1090/S0025-5718-10-02334-3

Thank you for your attention!
Any questions ?

e2s UPPA
energy environment solutions

Inria

UNIVERSITÉ DE PAU ET DES PAYS DE L'ADOUR

# Large Mach convergence



We work with relative $L^2$-errors

$$\mathcal{E}_p = \frac{\|p_h - \Pi p\|_{\mathcal{T}_h}}{\|\Pi p\|_{\mathcal{T}_h}}.$$

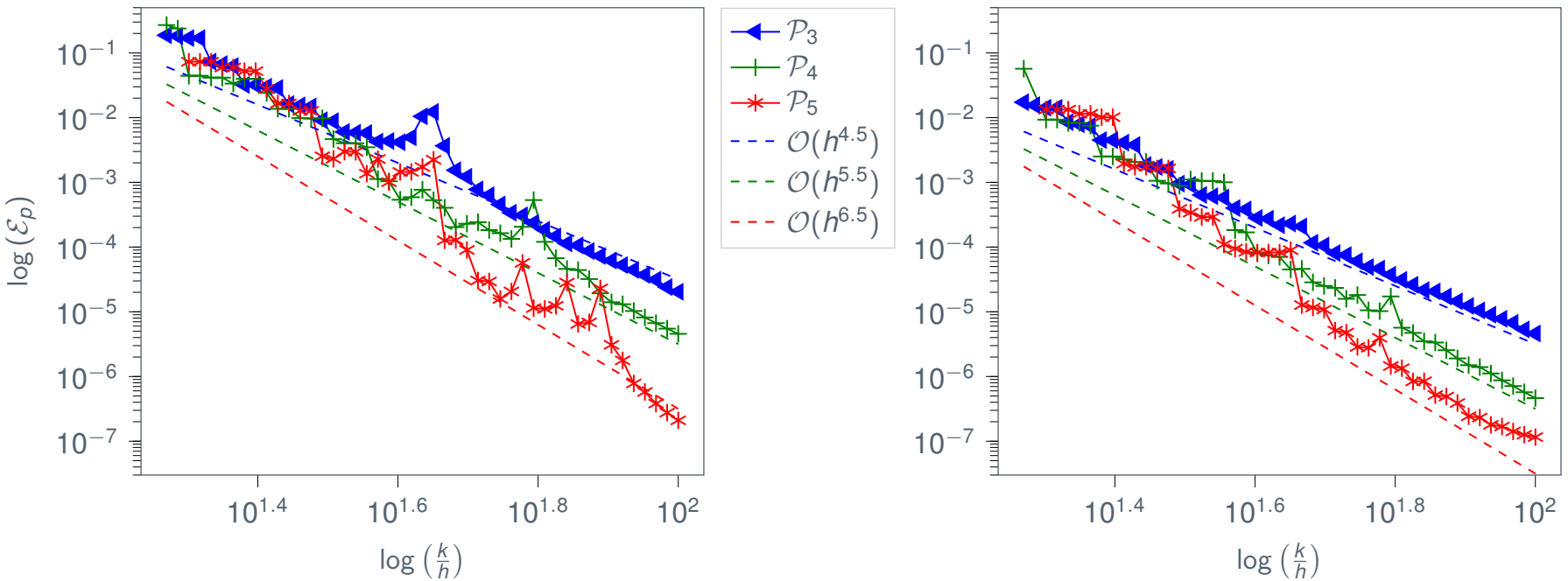


(a) HDG-$\boldsymbol{q}_h$ (b) HDG-$\boldsymbol{\sigma}_h$

Figure: Large Mach convergence for $p_h$

# Large Mach convergence



We work with relative $L^2$-errors

$$\mathcal{E}_p = \frac{\|p_h - \Pi p\|_{\mathcal{T}_h}}{\|\Pi p\|_{\mathcal{T}_h}}.$$

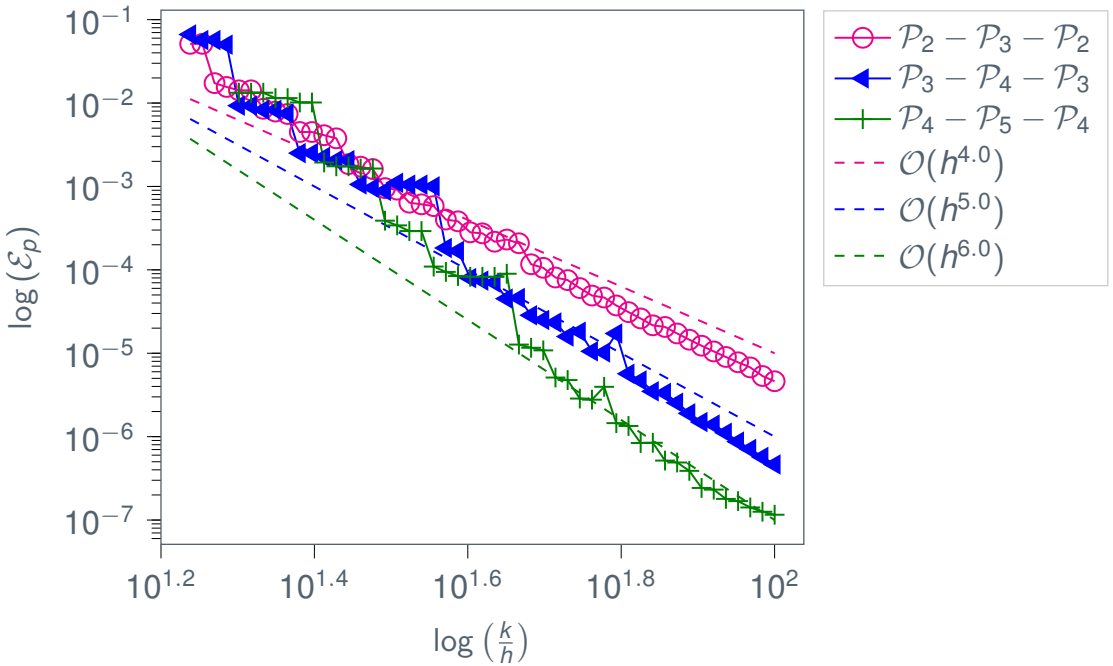


(a) HDG+

Figure: Large Mach convergence for $p_h$